

# Development of Electroplated Magnetic Materials for MEMS

Nosang V. Myung<sup>1</sup>, D.-Y. Park<sup>2</sup> and Paulo T. A. Sumodjo<sup>2,\*</sup>

<sup>1</sup>MEMS Technology Group, Jet Propulsion Laboratory,  
California Institute of Technology, Pasadena CA 91109

<sup>2</sup>Department of Chemical Engineering, University of California, Los Angeles CA 90095

## ABSTRACT

Soft ferromagnetic materials have thus far found the most utility in magnetic-MEMS, because the technologies necessary for depositing and micromachining them have been well developed previously by the data storage industry. However, hard magnetic materials have unique advantages that are driving their integration with MEMS. These include enhanced magnetic properties, corrosion resistance, electrical resistivity, and reduced films stress for electrodeposited soft and hard magnetic materials. The primary issues associated with the integration of these magnetic materials in MEMS are discussed.

## INTRODUCTION

Given the prohibitive cost of launching any payload into space (between \$10,000 - \$1000,000 per kg, depending on the type of mission), NASA's goal has been towards developing "smaller, faster and cheaper" space missions. Thus, "micro-spacecraft" (under 100 kg mass) enabled by integrated microdevices including inertial guidance devices, micro-propulsion devices, adaptive optics, micro-instruments and nano-mechanical resonator devices are of great interest. In this context, Micro/Nano Electro Mechanical Systems (MEMS/NEMS) technologies are exceptionally well suited for space applications because they offer the advantages of low mass, low power consumption and reliability, coupled with novel capabilities.

MEMS devices such microactuators, sensors, micromotors, and frictionless microgears require the use of both hard and soft magnetic materials because electromagnetically-actuated MEMS are more stable for high force and large actuation gap applications. Moreover, they are less susceptible to malfunction when subjected to adverse environments such as dust and humidity, and can be actuated with low cost voltage controllers (1-6).

There are many different ways to deposit and integrate magnetic materials into MEMS/NEMS. Electrochemical processes including electrodeposition and electroless deposition are well-suited to fulfill the requirements of high yield and cost effective processes. Electrochemical processes have many advantages, including precisely controlled room temperature operation, low energy requirements, rapid deposition rates, capability to handle complex geometries, low cost, and simple scale-up with easily

---

\* Visiting Scholar from Instituto de Química, Universidade de São Paulo, 05508-900 São Paulo, SP, Brasil.

maintained equipment. In addition, the properties of materials can be “tailored” by controlling solution compositions and deposition parameters. Due to these advantages, electroplated soft magnetic materials such as NiFe and CoNiFe have been widely used as recording head materials for computer hard drive industries (7). In the case of magnetic-MEMS/NEMS, the magnetic layer thickness can vary from a few nanometers to a few mm depending on the applications. Magnetic thin films must also have good adhesion, low-stress, corrosion resistance, and be thermally stable with excellent magnetic properties.

This paper reviews the currently available magnetic materials for MEMS/NEMS applications that can be produced by electrodeposition, and the challenges associated with the development of these materials. In addition, the dependence of the electrodeposited film properties on the various electroplating parameters including pH, temperature, metal ion concentration in the plating solution, complexing agents, other additives, current density (CD), hydrodynamics, and current waveforms (direct current, pulse plating, and pulse-reverse plating), will be discussed

## DISCUSSION

### Soft Magnetic Materials in MEMS

The most commonly used magnetic materials in MEMS are soft magnetic materials, such as permalloy (19%Ni-81%Fe alloy). The combination of relatively high magnetic saturation ( $M_S \approx 1$  T), low coercivity (low hysteresis loss), good corrosion resistance, and near zero magnetostriction (i.e. magnetic properties not affected by film stress) has led to the use of electrodeposited permalloy films in macroscopic and microscopic sensors, actuators, and systems. Perhaps the most significant application of permalloy in MEMS is in magnetic recording heads. The technologies necessary for the deposition and micromachining of permalloy are fairly well developed.

As the data storage density of computer drives increases dramatically (60 % per year), new, high-performance, soft magnetic materials are being considered and studied for possible use. Andriacos and Robertson reviewed the requirements for improved thin film recording heads (7). These include: 1) high magnetic saturation ( $M_S \gg 1$  T; currently thin film  $M_S$  is in the range of 2.3-2.4 T), 2) low coercivity ( $H_c < 1$  Oe), 3) optimal anisotropy field ( $H_k$ ) for high permeability ( $\mu$ ), 4) near zero magnetostriction ( $\lambda$ ), 5) high electrical resistivity ( $\rho$ ) and 6) good corrosion resistance.

Various CoFe and CoNi –based ternary and quaternary alloys have been considered for meeting the challenges of improved corrosion resistance, and lower film stress with superior soft magnetic properties. These electrodeposited alloys include CoFeB, CoFeCr, CoFeP, CoFeCu, CoNiFe, CoNiFeS, CoFeNiCr, CoFeSnP and CoNiFeB.

Magnetic Properties of Soft Magnetic Materials. Magnetic saturation of electrodeposited ferromagnetic materials is generally independent of electroplating conditions and only dependent on film composition. This is to be expected because  $M_S$  is an intrinsic material property. The highest magnetic saturation (up to 2.4 T) ever obtained experimentally was

for CoFe alloys with Fe compositions in the range from 55-78 %. Liao reported that electrodeposited CoFe alloys, especially 90Co10Fe, have promising magnetic properties, including high magnetic saturation (1.9 T), low coercivity (1 Oe) and near zero magnetostriction (8). However, those alloys exhibited very poor corrosion resistance and high film stress. CoNiFe alloys have attracted attention in the data storage industry due to their high magnetic saturation (upto 2.4 T). In addition, ternary 80Co10Ni10Fe electrodeposited films exhibit zero magnetostriction with  $M_S$  values around 1.6 T.

Figure 1 shows the magnetic saturation of NiFe, NiCo, CoFe, and CoNiFe films electrodeposited from chloride and sulfate baths (9,10). It is seen that for the Ni-based alloys, the magnetic saturation decreased linearly with increasing Ni content (fig. 1a). However, NiCo alloys exhibit higher  $M_S$  values for lower nickel content (approx. < 40 %). Both NiCo and NiFe alloys with Ni content greater than 40 % have practically the same values of magnetic saturation. These observations can be explained in terms of the change in structure of the films with increasing Ni content. Magnetic properties are extrinsic properties, and are thus influenced not only by film composition, but also by film stress, grain size, crystal structure, surface roughness, and film thickness. Osaka *et al.* observed that the coercivity of electrodeposited CoNiFe films from an electrolyte solution containing saccharin or thiourea additives (stress reducers or grain refiners) to be closely related to the sulfur content of the film (11). As it is seen in Fig. 1b, addition of Fe (up to 50 %) to both pure Co and CoNi thin films increases the  $M_S$  values sigmoidally from ~1.5 T (no Fe added) to a maximum of ~2.0 T. The addition of Ni in CoFe alloys however, has negligible effect on the magnetic saturation values. Varying impurity concentrations have been shown to result in slightly different magnetic saturation values for films with similar compositions. For example, higher  $M_S$  values of CoNiFe films were obtained using additive free electrolytes rather than electrolytes containing additives (e.g. saccharin).

Corrosion Resistance of Soft Magnetic Materials. Corrosion resistance or chemical stability of electrodeposited films is not only dependent on film composition, but is also a property of its crystal structure, grain size and impurity content. In general, among the iron group metals, nickel has the greatest corrosion resistance in acidic media, followed by cobalt. Iron is the most susceptible to corrosion. The corrosion resistance of iron group alloys decreases significantly with increasing Fe content. Ulhig explained this behavior via his electron configuration theory of passivity (12). According to this theory, the corrosion rate decreases substantially with increasing Ni content up to a critical composition of 34 % Ni. For Ni contents greater than 34%, the corrosion behavior of the alloy is approximately that of the pure nickel phase.

In NiFe alloys, the corrosion resistance of the Ni-rich fcc phase is an order of magnitude higher than that for the Fe-rich bcc phases. 50Ni50Fe deposits exhibited the greatest corrosion resistance, probably due to the smaller grain sizes. Similarly, the Co-rich hcp phase of CoNi alloys has an order of magnitude lower corrosion resistance than the Ni-rich fcc phase. Nanocrystalline fcc 70Ni30Co deposits exhibited the highest corrosion resistance for CoNi alloys. The corrosion resistance of CoFe alloys are an order of magnitude lower than that for fcc NiFe and fcc CoNi alloys. Substantial improvements in corrosion resistance are obtained by the addition of Ni to electrodeposited CoFe alloys. Conversely, the addition of B has only a slight effect on the corrosion resistance. Figure 2

shows the comparison of the corrosion resistances of iron group alloys after 1 hour of immersion in 0.5 M NaCl (9).

Electrodeposited films are more susceptible to corrosion than physical vapor deposited films or bulk alloys because the presence of organic additives (e.g. saccharin or thiourea) in the electrodeposition bath can cause anodic attack and prevent the formation of a passive film (13).

Electrical Resistivity of Soft Magnetic Materials. A consequence of the drive for increasing data rates in data storage industry and for applications in RF MEMS is the requirement for faster switching of magnetic materials. Rapid magnetic field switching results in the formation of eddy currents, which can dramatically reduce the effective permeability of magnetic films during high frequency operation. Two different approaches, the use of multilayered structures and increasing film resistance via impurity incorporation, were proposed to minimize eddy currents (7, 14). Yokoshima et al. (14) observed an increase in electrical resistivity from approximately 20 to 130  $\mu\Omega$  cm with the addition of DET (up to 20 g/L) into the plating solution. This effect was attributed to carbon incorporation with the films, resulting in increased impurity-based electron scattering and a change in microstructure (14). However, increases in electrical resistivity via impurity incorporation can be detrimental by also decreasing the magnetic saturation of the material.

Figure 3 shows the electrical resistivity of electrodeposited NiFe and CoNi thin films and for comparison, the electrical resistivity of bulk CoNi alloys. It is seen that the electrical resistivity of electrodeposited NiFe alloys decreases monotonically with increasing Ni content from 40 to 100 % Ni. The electrical resistivity of NiFe films (thickness  $\geq 1$   $\mu\text{m}$ ) with high Fe content ( $>40$  %) is difficult to measure due to the formation of stressed, cracked deposits. In contrast, the electrical resistivity of both electrodeposited and bulk CoNi alloys remains practically constant, around 10  $\mu\Omega$  cm, for Ni contents below 40 %. For bulk CoNi alloys with higher Ni contents, the resistivity increases slightly with increasing Ni content, exhibiting a maximum at about 70 % Ni. Electrodeposited CoNi alloys also show the same trend (with a maximum around 80 % Ni). However, the resistivity of electrodeposited alloys are considerably higher in comparison to bulk alloys. This higher electrical resistivity of the electrodeposited CoNi alloys can be attributed to the smaller grain sizes, high defect densities, and impurity incorporation during electrodeposition.

Residual Stress of Soft Magnetic Materials. Residual stress in the electrodeposited films is an important factor for MEMS devices because, unlike in the data storage application, the thickness of magnetic films in MEMS can range from nanometers (e.g. NEMS devices) to few millimeters thick (e.g. LIGA devices). In many cases, this film stress could exceed the strength of the film, resulting in cracking, deformation of devices, and interfacial failure.

Two kinds of film stress exist in electrodeposited materials: differential thermal stress and residual stress. Thermal stress occurs as a consequence of high temperature electrodeposition or of heating of the bath during electrodeposition. The magnitude of the stress can be calculated by knowing the thermal expansion coefficients of the

electrodeposited material and the substrate respectively, and can be minimized by optimizing the electrodeposition conditions at temperatures closer to room temperature. Residual stress, on the other hand, is defined as the stress within the electrodeposited material, which does not arise from mechanical loading or temperature gradients, but yet remains in internal equilibrium (15). Many factors contribute to the development of residual stress in deposits, including film composition, nature of the substrate surface and of the deposit, solution composition (metal ion concentration, pH, complexing agent, additives, anions), temperature, current density, current waveform, agitation, and the deposit thickness. Dini (15) observed that in electrodeposited transition metals, which exhibit the highest residual stress values, there is an apparent relationship between the stress and the melting points of these metals. Generally, a high residual stress is observed at the beginning of the electrodeposition, reaching a constant value for thicknesses in the range of 12.5 to 25  $\mu\text{m}$ . The high initial intrinsic stress in the deposit is associated with lattice mismatch and with the grain size of the underlying substrate.

Since there are many parameters affecting the stress of deposits, deposition conditions must be optimized on an individual basis. Figure 4 shows the effect of current density on the residual stress and surface morphology of nickel electrodeposits from sulfamate baths. Lower current densities lead to the formation of stressed deposits. With increasing current density, stress tends to level out. From figure 4b it can be seen that the morphology of the film is also highly dependent on the applied current density.

Best-known stress reducing agents for nickel electrodeposition are sulfur containing organic additives (e.g. saccharin, thiourea, aminobenzene sulfonic acid, benzene sulfamide, benzene sulfonic acid, etc). Thiourea also influences the residual stress in cobalt electrodeposits. Slightly compressive cobalt films were obtained using a plating solution containing 25 to 50 mg/L thiourea (16). These sulfur containing organic additives suffer decomposition on the substrate surface and the products are partially incorporated in the deposit (e.g. sulfur, carbon, or both). Figure 5 shows the effect of saccharin concentration on the residual stress of Ni, 85Co15Ni, and 65Co15Ni20Fe films ( residual stress data for the 65Co15Ni20Fe film is taken from literature (18)). Small additions of saccharin to plating solutions can alter the residual stress of nickel from tensile to compressive.

### Hard Magnetic Materials in MEMS

Although soft magnetic materials can be used to produce high-force actuators and sensitive magnetometers, hard magnetic or permanent magnetic materials would be more appropriate in some cases. For example, hard magnetic materials with a high remanence,  $M_r$ , are well suited for bi-directional (push-pull) microactuator applications (17). In addition, microactuators driven by off-chip coils can be activated with lower fields and hence lower power levels if a hard magnetic material is used instead of a soft magnetic material. However, except in a few cases, hard magnetic materials have not been used extensively in MEMS (6). The primary reason for this is the lack of readily available and reliable deposition and micromachining processes. A large variety of hard magnetic materials can be prepared by metallurgical processes (e.g. sintering, pressure bonding, injection molding, casting, extruding, and calendaring), vacuum processes (e.g.

evaporation, sputtering, MBE, CVD) and electrochemical processes (e.g. electroless deposition and electrodeposition).

Magnetic Properties of Hard Magnetic Materials. To date, most hard magnetic materials have been alloys based on cobalt because its hcp crystalline structure is highly anisotropic. Electrochemically, Co-based alloys containing P, As, Sb, Bi, W, Cr, Mo, Pd, Pt, Ni, Fe, Cu, Mn, O and H have been deposited. Alloying elements tend to concentrate at the grain boundaries. Thus, the resulting structure consists of isolated magnetic Co grains surrounded by non-magnetic or weakly magnetic boundaries (19). Such microstructural formations increase the energy barrier for magnetic realignment of the domains and thereby increase the overall coercivity  $H_C$  of the films, making them magnetically hard. Park et al. observed that the addition of phosphorus into electrodeposited CoNi films produced nanocrystalline films with a modified crystal structure, increasing the energy barriers required for the magnetic alignment of the CoNi grains (20). Elements that are exceptions to this rule are Pd and Pt, which are readily alloyed with Co or CoNi and instead have the effect of increasing the magnetocrystalline anisotropy (21). Luborsky's experiments with electrodeposited Co and CoNi containing P, As, Sb, Bi, W, Mo and Cr as alloying elements showed that the concentration of the alloying element required for maximum coercivity decreased in the following orders  $P > As > Sb > Bi$  and  $W > Mo > Cr$  (19). Also, as expected, the magnetic saturation  $M_S$ , decreases with increasing content of the non-magnetic alloying element. Low alloy concentrations of phosphorus and tungsten, however, have resulted in films with high coercivity with yet having relatively high  $M_S$ .

Promising hard magnetic thin film materials include CoPt and FePt due to their high magnetocrystalline anisotropy and magnetic saturation (21). Specifically,  $L_{10}$  ordered phase materials (Co<sub>50</sub>Pt<sub>50</sub> and Fe<sub>50</sub>Pt<sub>50</sub>) show extremely high coercivities ( $>10,000$  Oe) (22). Most investigations of CoPt and FePt magnetic thin films were conducted using vacuum-based processes [e.g. MBE (23) and sputtering (22-25)], in which CoPt and FePt were deposited as multilayered structures and then annealed to produce ordered phases. A major disadvantage of these deposition methods for some magnetic MEMS applications is the requirement for high-temperature post-annealing processes (e.g. 500-700 °C). Integrated circuits and some materials commonly used in MEMS (e.g. Al, polymer, etc.) do not survive at these temperatures. Although Farrow and Marks report that by electrochemically charging the transition metal alloy films with hydrogen, one can minimize the effects of the annealing process (25), it is nevertheless still a problem.

CoPt and Co/Pt multilayers can be electrodeposited from various plating solutions at or near room temperature (26-30). Cavallotti et al obtained hard magnetic Co-Pt electrodeposits with a coercivity that ranged from 4000 to 2000 Oe for film thicknesses from 50 nm to 10 microns (30).

Myung *et al.* also studied various electrodeposited hard magnetic Co-based alloys and found promising hard magnetic properties. Coercivity in the direction parallel to the film decreased in the following sequence: CoPtP  $>$  CoNiP  $\approx$  CoP  $>$  CoMnP  $>$  CoW. In the perpendicular direction, coercivity decreased in the sequence of CoPtP  $>$  CoNiP  $\approx$  CoMnP  $>$  CoP  $>$  Co/Cu multilayers  $>$  CoW (31). Figure 6 shows how the coercivity of different phosphorus containing alloys varies with the P content. Non-Ni containing

alloys, such as CoP, exhibit increasing coercivity with increasing P incorporation into the alloy. On the other hand, Ni containing alloys show this increase in coercivity with increasing amount of P in the alloy, only for low P concentrations. As more phosphorus is added to these alloys, the coercivity reaches a maximum, followed by a significant reduction at high P concentrations. The highest coercivities were observed for the 85Co15NiP films. Figure 7 shows the hysteresis loops (fig. 7a) and 2<sup>nd</sup> quadrant B-H curves (fig. 7b) for these various electrodeposited alloys.

Corrosion Resistance of Hard Magnetic Materials. As shown in Figure 2, electrodeposited cobalt is much more susceptible to corrosion attack than either nickel or permalloy. Non-magnetic alloying elements (e.g. phosphorus, tungsten, manganese) are not beneficial in this respect and can significantly lower the corrosion resistance of these alloys. Furthermore, it has been observed that some of these hard magnetic materials are etched away during the photoresist removal step during lithographic patterning. It is therefore recommended that these magnetic materials have an overcoat of high corrosion resistance materials (e.g. Au, Pt, Ni) in order to prevent their dissolution during MEMS processing.

Residual Stress of Hard Magnetic Materials. In general, hard magnetic alloys become mechanically brittle and hard as their magnetic hardness increases. Therefore, this reduction in mechanical ductility results also in hard magnetic materials having high residual stress. Figure 8 shows the residual stress of electrodeposited CoNiP and CoP films plotted as a function of the P content. Electrodeposited CoNiP and CoP films have a much higher (above 200 MPa) tensile residual stress than pure nickel or cobalt films and show a maximum in the residual stress when the electrolyte baths concentrations of NaH<sub>2</sub>PO<sub>2</sub> are in the range of 1 to 2 g/L. In order to lower the residual stress while yet maintaining high coercivity, composite films consisting of these highly tensile magnetic films sandwiched between compressive films can be electrodeposited.

## CONCLUSION

Magnetic materials, particularly ferromagnetic materials, have many uses in MEMS. Although soft magnetic materials have found the greatest utility in MEMS, improved processes for integrating hard magnetic materials with MEMS are being developed. These electrochemical processes and resulting properties of the deposited magnetic films must be further optimized for use in high-force microactuators and low-power microsensors.

## ACKNOWLEDGEMENT

The authors wish to acknowledge his collaborators, including T. George, D. Wiberg, K.-ah Son, B. Eyre, O. Orient, D. Miller from JPL and K. Nobe, M. Schwartz, B.-Y. Yoo and J.W. Judy from UCLA. This work was supported by the NASA Code-R and DARPA MEMS Program DABT63-99-1-0020.

## REFERENCES

1. J. W. Judy, R. S. Muller and H. H. Zappe, *IEEE J. Microelectromechanical Systems*, **4**, 162 (1995).

2. J. W. Judy and R. S. Muller, *Sensors and Actuators (Physical A)*, **A53**, 392 (1996).
3. J. W. Judy and R. S. Muller, *IEEE J. Microelectromechanical Sys.*, **6**, 249 (1997).
4. C. H. Ahn and M. G. Allen, *IEEE Trans. Ind. Electron.* **45**, 866 (1998).
5. T. M. Liakopoulos, M. Xu and C. H. Ahn, *Technical Digest Solid-State Sensor and Actuator Workshop*, Hilton Head Island, SC, USA, 19 (1998).
6. T. S. Chin, *J. Magn. Magn. Mater.* **209**, 75 (2000).
7. P. C. Andricacos and N. Robertson, *IBM J. Res. Develop.*, **42** 671 (1998).
8. S.H. Liao, *IEEE Trans. Mag.*, **26**, 328 (1998).
9. N. V. Myung and K. Nobe, *J. Electrochem. Soc.* **148**, C133 (2001).
10. D. Kim, D.-Y. Park, B.Y. Yoo, P.T.A. Sumodjo and N.V. Myung, *Electrochim. Acta*, *in press* (2002).
11. T. Osaka, T. Sawaguchi, F. Mizutani, T. Yokoshina, *J. Electrochem. Soc.*, **146**, 3295 (1999).
12. H.H. Uhlig, "*Corrosion Handbook*" John Wiley and Sons, Inc., pp. 194 (1948).
13. G. S. Frankel, V. Brusica, R. G. Schad and J. -W. Chang, *Corr. Sci.*, **35**, 63 (1993).
14. T. Yokoshima, M. Kaseda, M. Yamada, T. Nakanishi, T. Momma, T. Osaka, *IEEE Trans. Magn.* **35**, 2499 (1999).
15. J. W. Dini, "*Electrodeposition - The Materials Science of Coating and Substrates*", Chap. 9, Noyes Publications, (1992).
16. Yu. K. Vyagis, A. I. Bodnevas, and Yu. Matulis, *Protection of Metals*, **1**, 468 (1965).
17. I. Tabakovic, V. Inturi, S. Riemer, *J. Electrochem. Soc.*, **149**, C18 (2002).
18. H. J. Cho, S. Bhansali, and C. H. Ahn, *J. Appl. Phys.*, **87**, 6340 (2000).
19. F. E. Luborsky, *IEEE Tran. Magn.*, **6**, 502 (1970).
20. D.-Y. Park, N.V. Myung, M. Schwartz, and K. Nobe, *Electrochim. Acta*, **47**, 2893 (2002).
21. R. M. Bozorth, *Ferromagnetism*, D. Van Nostrand (1963).
22. K. R. Coffey, M. A. Parker and J. K. Howard, *IEEE Trans Magn.* **31**, 2737 (1995).
23. C. H. Lee, R. F. C. Farrow, C. J. Lin and E. E. Marinero, *Phys Rev. B.* **42**(7) 11384 (1990).
24. P. F. Garcia, Z. G. Li, and W. B. Zeper, *J. Magn. Magn. Mater.*, **121**, 452 (1993).
25. R. F. Farrow and R. F. Marks, *U. S. Patent #5,792,510*.
26. Y. Jyoko, S. Kashiwabara, Y. Hayashi, W. Schwarzacher, *J. Magn. Magn. Mater.*, **198/99**, 239 (1999).
27. J. Horkans, D. J. Seagle, and C. H. Chang, *J. Electrochem. Soc.*, **137**, 2056 (1990).
28. M. Monew, I. Krastev, and A. Zielonka, *J. Phys. Cond. Matter*, **49**, 10033 (1999).
29. V. Tutovan and V. Georgescu, *Thin Solid Films*, **61**, 133 (1970).
30. P. L. Cavallotti, N. Lecis, H. Fauser, A. Zielonka, J. P. Celis, G. Wouters, J. Machado da Silva, J. M.B. Oliveira and M. A. Sa, *Surf. Coat. Technol.*, **105**, 232 (1998).
31. N. V. Myung, D.-Y. Park, M. Schwartz, K. Nobe, H. Yang, C.-K. Yang, J. W. Judy, *Proc. Electrochemical Soc.* **PV2000-29**, 506 (2000).



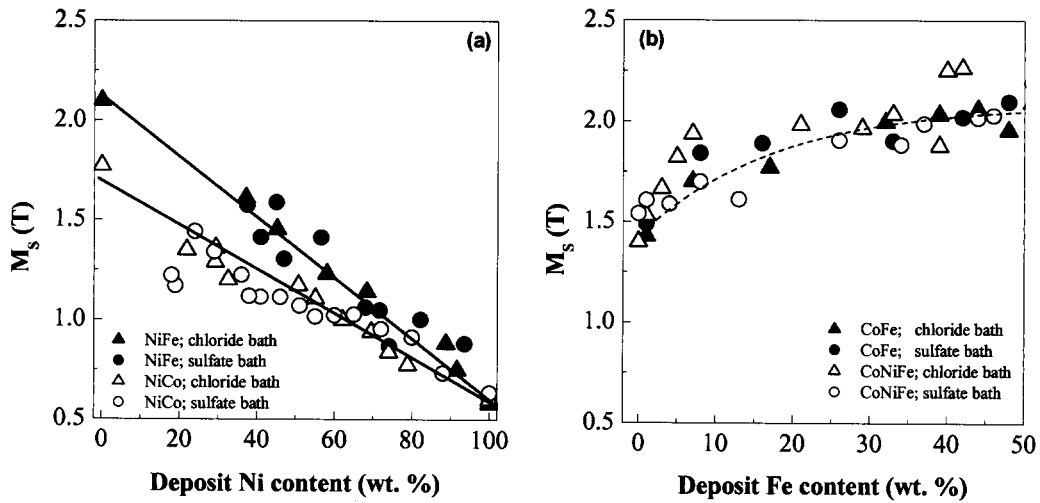


**Figure 1.** Magnetic Saturation of electrodeposited (a) NiFe, NiCo, and (b) CoFe, and CoNiFe films [Ref. 8,9].

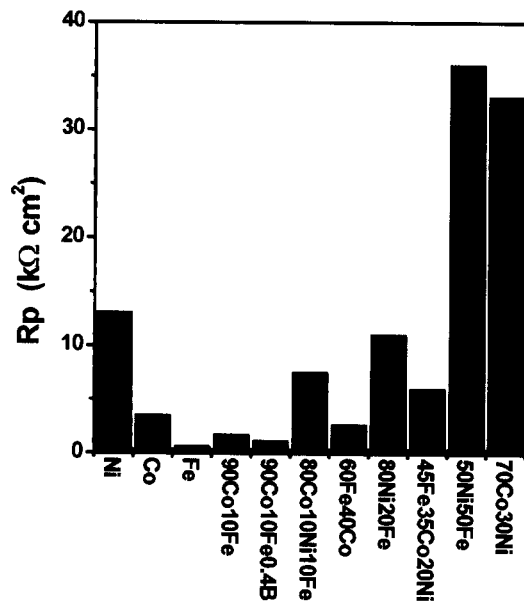


**Figure 2.** Comparison of corrosion resistances of iron group alloys in 0.5 M NaCl after 1 hour immersion.

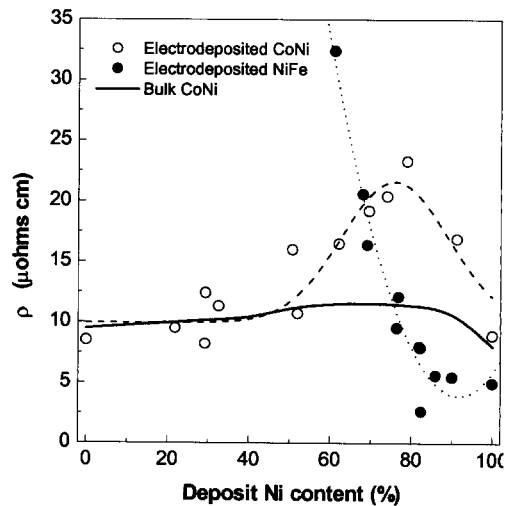


**Figure 3.** Electrical resistivity of NiFe and CoNi thin films electrodeposited from chloride baths and bulk CoNi.

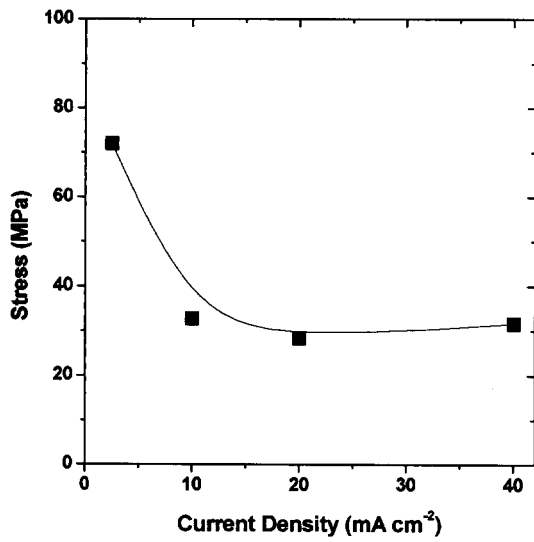


**Figure 4a.** Intrinsic stress of electrodeposited Ni from 1 M Ni sulfamate bath, pH = 4.0, Temp = 60 °C.

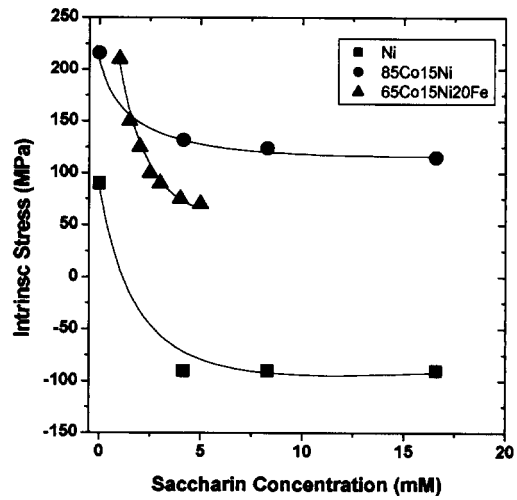


**Figure 5.** Residual stress of electrodeposited Ni, 85Co15Ni, and 65Co15Ni20Fe films. Ni and 85Co15Ni were electrodeposited from sulfamate baths, 65Co15Ni20Fe film data is from literature (17).

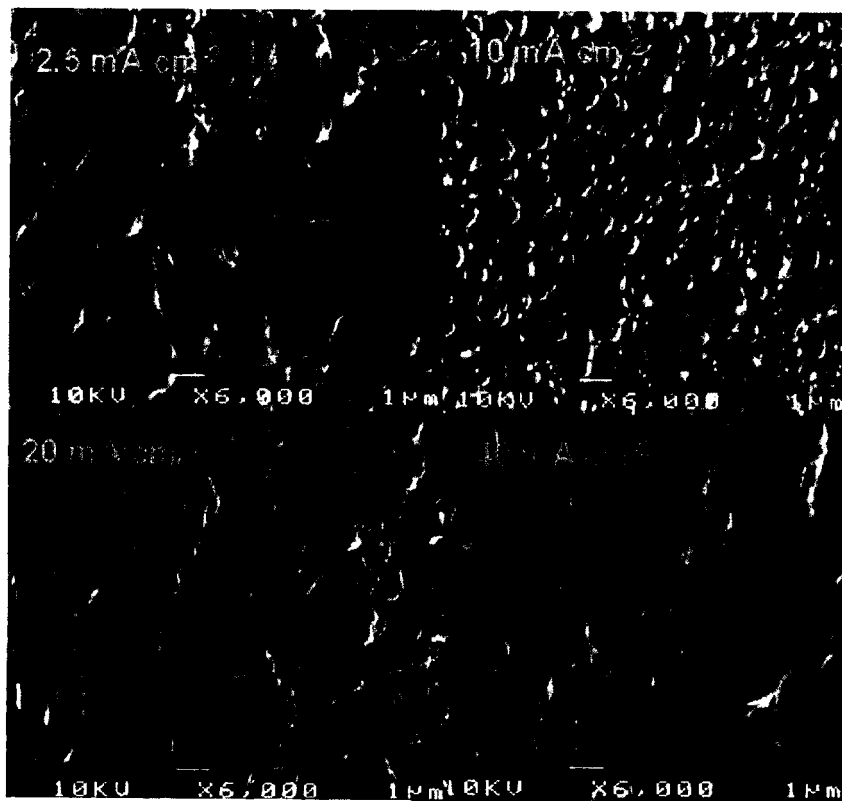


**Figure 4b.** SEM micrographs of Ni films electrodeposited from a 1 M Ni sulfamate bath, pH = 4.0, Temp = 60 °C.

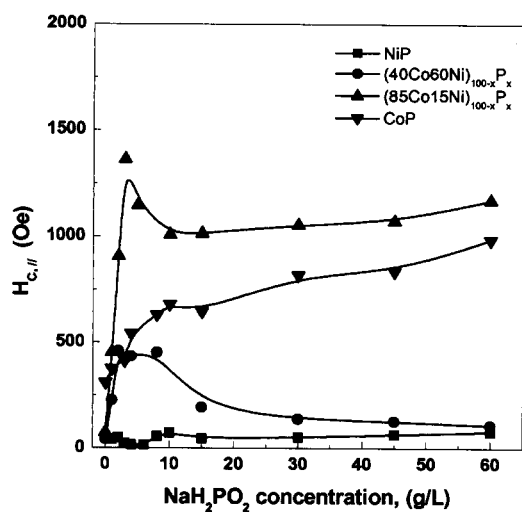


**Figure 6.** Coercivity of electrodeposited NiP 40Co60NiP, 85Co15NiP and CoP films: All films were electrodeposited from chloride baths.

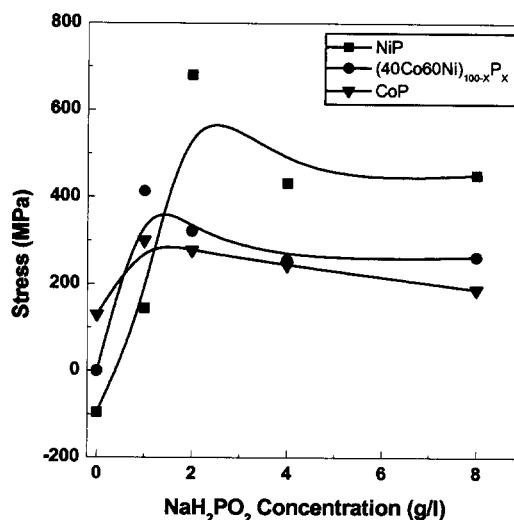
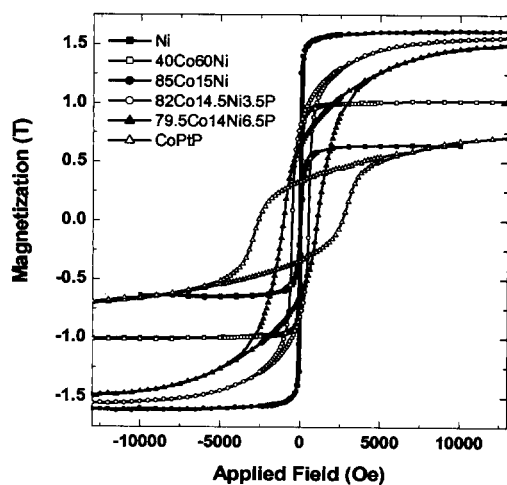


**Figure 8.** Residual stress of electrodeposited NiP 40Co60NiP, and CoP films: All films were electrodeposited from chloride baths.

a)



b)

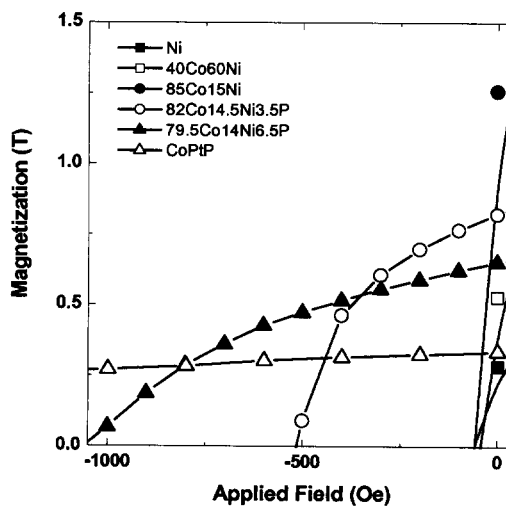


**Figure 7.** Hysteresis loop (a) and 2<sup>nd</sup> quadrant B-H curves for various electrodeposited magnetic alloys

# Development of Electroplated Magnetic Materials for MEMS

Nosang V. Myung<sup>1</sup>, D.-Y. Park<sup>2</sup> and Paulo T. A. Sumodjo<sup>2,\*</sup>

<sup>1</sup>MEMS Technology Group, Jet Propulsion Laboratory,  
California Institute of Technology, Pasadena CA 91109

<sup>2</sup>Department of Chemical Engineering, University of California, Los Angeles CA 90095

## ABSTRACT

Soft ferromagnetic materials have thus far found the most utility in magnetic-MEMS, because the technologies necessary for depositing and micromachining them have been well developed previously by the data storage industry. However, hard magnetic materials have unique advantages that are driving their integration with MEMS. These include enhanced magnetic properties, corrosion resistance, electrical resistivity, and reduced films stress for electrodeposited soft and hard magnetic materials. The primary issues associated with the integration of these magnetic materials in MEMS are discussed.

## INTRODUCTION

Given the prohibitive cost of launching any payload into space (between \$10,000 - \$1000,000 per kg, depending on the type of mission), NASA's goal has been towards developing "smaller, faster and cheaper" space missions. Thus, "micro-spacecraft" (under 100 kg mass) enabled by integrated microdevices including inertial guidance devices, micro-propulsion devices, adaptive optics, micro-instruments and nano-mechanical resonator devices are of great interest. In this context, Micro/Nano Electro Mechanical Systems (MEMS/NEMS) technologies are exceptionally well suited for space applications because they offer the advantages of low mass, low power consumption and reliability, coupled with novel capabilities.

MEMS devices such microactuators, sensors, micromotors, and frictionless microgears require the use of both hard and soft magnetic materials because electromagnetically-actuated MEMS are more stable for high force and large actuation gap applications. Moreover, they are less susceptible to malfunction when subjected to adverse environments such as dust and humidity, and can be actuated with low cost voltage controllers (1-6).

There are many different ways to deposit and integrate magnetic materials into MEMS/NEMS. Electrochemical processes including electrodeposition and electroless deposition are well-suited to fulfill the requirements of high yield and cost effective processes. Electrochemical processes have many advantages, including precisely controlled room temperature operation, low energy requirements, rapid deposition rates, capability to handle complex geometries, low cost, and simple scale-up with easily

---

\* Visiting Scholar from Instituto de Química, Universidade de São Paulo, 05508-900 São Paulo, SP, Brasil.

maintained equipment. In addition, the properties of materials can be “tailored” by controlling solution compositions and deposition parameters. Due to these advantages, electroplated soft magnetic materials such as NiFe and CoNiFe have been widely used as recording head materials for computer hard drive industries (7). In the case of magnetic-MEMS/NEMS, the magnetic layer thickness can vary from a few nanometers to a few mm depending on the applications. Magnetic thin films must also have good adhesion, low-stress, corrosion resistance, and be thermally stable with excellent magnetic properties.

This paper reviews the currently available magnetic materials for MEMS/NEMS applications that can be produced by electrodeposition, and the challenges associated with the development of these materials. In addition, the dependence of the electrodeposited film properties on the various electroplating parameters including pH, temperature, metal ion concentration in the plating solution, complexing agents, other additives, current density (CD), hydrodynamics, and current waveforms (direct current, pulse plating, and pulse-reverse plating), will be discussed

## DISCUSSION

### Soft Magnetic Materials in MEMS

The most commonly used magnetic materials in MEMS are soft magnetic materials, such as permalloy (19%Ni-81%Fe alloy). The combination of relatively high magnetic saturation ( $M_s \approx 1$  T), low coercivity (low hysteresis loss), good corrosion resistance, and near zero magnetostriction (i.e. magnetic properties not affected by film stress) has led to the use of electrodeposited permalloy films in macroscopic and microscopic sensors, actuators, and systems. Perhaps the most significant application of permalloy in MEMS is in magnetic recording heads. The technologies necessary for the deposition and micromachining of permalloy are fairly well developed.

As the data storage density of computer drives increases dramatically (60 % per year), new, high-performance, soft magnetic materials are being considered and studied for possible use. Andriacos and Robertson reviewed the requirements for improved thin film recording heads (7). These include: 1) high magnetic saturation ( $M_s \gg 1$  T; currently thin film  $M_s$  is in the range of 2.3-2.4 T), 2) low coercivity ( $H_c < 1$  Oe), 3) optimal anisotropy field ( $H_k$ ) for high permeability ( $\mu$ ), 4) near zero magnetostriction ( $\lambda$ ), 5) high electrical resistivity ( $\rho$ ) and 6) good corrosion resistance.

Various CoFe and CoNi –based ternary and quaternary alloys have been considered for meeting the challenges of improved corrosion resistance, and lower film stress with superior soft magnetic properties. These electrodeposited alloys include CoFeB, CoFeCr, CoFeP, CoFeCu, CoNiFe, CoNiFeS, CoFeNiCr, CoFeSnP and CoNiFeB.

Magnetic Properties of Soft Magnetic Materials. Magnetic saturation of electrodeposited ferromagnetic materials is generally independent of electroplating conditions and only dependent on film composition. This is to be expected because  $M_s$  is an intrinsic material property. The highest magnetic saturation (up to 2.4 T) ever obtained experimentally was

for CoFe alloys with Fe compositions in the range from 55-78 %. Liao reported that electrodeposited CoFe alloys, especially 90Co10Fe, have promising magnetic properties, including high magnetic saturation (1.9 T), low coercivity (1 Oe) and near zero magnetostriction (8). However, those alloys exhibited very poor corrosion resistance and high film stress. CoNiFe alloys have attracted attention in the data storage industry due to their high magnetic saturation (upto 2.4 T). In addition, ternary 80Co10Ni10Fe electrodeposited films exhibit zero magnetostriction with  $M_S$  values around 1.6 T.

Figure 1 shows the magnetic saturation of NiFe, NiCo, CoFe, and CoNiFe films electrodeposited from chloride and sulfate baths (9,10). It is seen that for the Ni-based alloys, the magnetic saturation decreased linearly with increasing Ni content (fig. 1a). However, NiCo alloys exhibit higher  $M_S$  values for lower nickel content (approx. < 40 %). Both NiCo and NiFe alloys with Ni content greater than 40 % have practically the same values of magnetic saturation. These observations can be explained in terms of the change in structure of the films with increasing Ni content. Magnetic properties are extrinsic properties, and are thus influenced not only by film composition, but also by film stress, grain size, crystal structure, surface roughness, and film thickness. Osaka *et al.* observed that the coercivity of electrodeposited CoNiFe films from an electrolyte solution containing saccharin or thiourea additives (stress reducers or grain refiners) to be closely related to the sulfur content of the film (11). As it is seen in Fig. 1b, addition of Fe (up to 50 %) to both pure Co and CoNi thin films increases the  $M_S$  values sigmoidally from ~1.5 T (no Fe added) to a maximum of ~2.0 T. The addition of Ni in CoFe alloys however, has negligible effect on the magnetic saturation values. Varying impurity concentrations have been shown to result in slightly different magnetic saturation values for films with similar compositions. For example, higher  $M_S$  values of CoNiFe films were obtained using additive free electrolytes rather than electrolytes containing additives (e.g. saccharin).

Corrosion Resistance of Soft Magnetic Materials. Corrosion resistance or chemical stability of electrodeposited films is not only dependent on film composition, but is also a property of its crystal structure, grain size and impurity content. In general, among the iron group metals, nickel has the greatest corrosion resistance in acidic media, followed by cobalt. Iron is the most susceptible to corrosion. The corrosion resistance of iron group alloys decreases significantly with increasing Fe content. Uhlig explained this behavior via his electron configuration theory of passivity (12). According to this theory, the corrosion rate decreases substantially with increasing Ni content up to a critical composition of 34 % Ni. For Ni contents greater than 34%, the corrosion behavior of the alloy is approximately that of the pure nickel phase.

In NiFe alloys, the corrosion resistance of the Ni-rich fcc phase is an order of magnitude higher than that for the Fe-rich bcc phases. 50Ni50Fe deposits exhibited the greatest corrosion resistance, probably due to the smaller grain sizes. Similarly, the Co-rich hcp phase of CoNi alloys has an order of magnitude lower corrosion resistance than the Ni-rich fcc phase. Nanocrystalline fcc 70Ni30Co deposits exhibited the highest corrosion resistance for CoNi alloys. The corrosion resistance of CoFe alloys are an order of magnitude lower than that for fcc NiFe and fcc CoNi alloys. Substantial improvements in corrosion resistance are obtained by the addition of Ni to electrodeposited CoFe alloys. Conversely, the addition of B has only a slight effect on the corrosion resistance. Figure 2

shows the comparison of the corrosion resistances of iron group alloys after 1 hour of immersion in 0.5 M NaCl (9).

Electrodeposited films are more susceptible to corrosion than physical vapor deposited films or bulk alloys because the presence of organic additives (e.g. saccharin or thiourea) in the electrodeposition bath can cause anodic attack and prevent the formation of a passive film (13).

Electrical Resistivity of Soft Magnetic Materials. A consequence of the drive for increasing data rates in data storage industry and for applications in RF MEMS is the requirement for faster switching of magnetic materials. Rapid magnetic field switching results in the formation of eddy currents, which can dramatically reduce the effective permeability of magnetic films during high frequency operation. Two different approaches, the use of multilayered structures and increasing film resistance via impurity incorporation, were proposed to minimize eddy currents (7, 14). Yokoshima et al. (14) observed an increase in electrical resistivity from approximately 20 to 130  $\mu\Omega$  cm with the addition of DET (up to 20 g/L) into the plating solution. This effect was attributed to carbon incorporation with the films, resulting in increased impurity-based electron scattering and a change in microstructure (14). However, increases in electrical resistivity via impurity incorporation can be detrimental by also decreasing the magnetic saturation of the material.

Figure 3 shows the electrical resistivity of electrodeposited NiFe and CoNi thin films and for comparison, the electrical resistivity of bulk CoNi alloys. It is seen that the electrical resistivity of electrodeposited NiFe alloys decreases monotonically with increasing Ni content from 40 to 100 % Ni. The electrical resistivity of NiFe films (thickness  $\geq 1$   $\mu\text{m}$ ) with high Fe content ( $>40$  %) is difficult to measure due to the formation of stressed, cracked deposits. In contrast, the electrical resistivity of both electrodeposited and bulk CoNi alloys remains practically constant, around 10  $\mu\Omega$  cm, for Ni contents below 40 %. For bulk CoNi alloys with higher Ni contents, the resistivity increases slightly with increasing Ni content, exhibiting a maximum at about 70 % Ni. Electrodeposited CoNi alloys also show the same trend (with a maximum around 80 % Ni). However, the resistivity of electrodeposited alloys are considerably higher in comparison to bulk alloys. This higher electrical resistivity of the electrodeposited CoNi alloys can be attributed to the smaller grain sizes, high defect densities, and impurity incorporation during electrodeposition.

Residual Stress of Soft Magnetic Materials. Residual stress in the electrodeposited films is an important factor for MEMS devices because, unlike in the data storage application, the thickness of magnetic films in MEMS can range from nanometers (e.g. NEMS devices) to few millimeters thick (e.g. LIGA devices). In many cases, this film stress could exceed the strength of the film, resulting in cracking, deformation of devices, and interfacial failure.

Two kinds of film stress exist in electrodeposited materials: differential thermal stress and residual stress. Thermal stress occurs as a consequence of high temperature electrodeposition or of heating of the bath during electrodeposition. The magnitude of the stress can be calculated by knowing the thermal expansion coefficients of the

electrodeposited material and the substrate respectively, and can be minimized by optimizing the electrodeposition conditions at temperatures closer to room temperature. Residual stress, on the other hand, is defined as the stress within the electrodeposited material, which does not arise from mechanical loading or temperature gradients, but yet remains in internal equilibrium (15). Many factors contribute to the development of residual stress in deposits, including film composition, nature of the substrate surface and of the deposit, solution composition (metal ion concentration, pH, complexing agent, additives, anions), temperature, current density, current waveform, agitation, and the deposit thickness. Dini (15) observed that in electrodeposited transition metals, which exhibit the highest residual stress values, there is an apparent relationship between the stress and the melting points of these metals. Generally, a high residual stress is observed at the beginning of the electrodeposition, reaching a constant value for thicknesses in the range of 12.5 to 25  $\mu\text{m}$ . The high initial intrinsic stress in the deposit is associated with lattice mismatch and with the grain size of the underlying substrate.

Since there are many parameters affecting the stress of deposits, deposition conditions must be optimized on an individual basis. Figure 4 shows the effect of current density on the residual stress and surface morphology of nickel electrodeposits from sulfamate baths. Lower current densities lead to the formation of stressed deposits. With increasing current density, stress tends to level out. From figure 4b it can be seen that the morphology of the film is also highly dependent on the applied current density.

Best-known stress reducing agents for nickel electrodeposition are sulfur containing organic additives (e.g. saccharin, thiourea, aminobenzene sulfonic acid, benzene sulfamide, benzene sulfonic acid, etc). Thiourea also influences the residual stress in cobalt electrodeposits. Slightly compressive cobalt films were obtained using a plating solution containing 25 to 50 mg/L thiourea (16). These sulfur containing organic additives suffer decomposition on the substrate surface and the products are partially incorporated in the deposit (e.g. sulfur, carbon, or both). Figure 5 shows the effect of saccharin concentration on the residual stress of Ni, 85Co15Ni, and 65Co15Ni20Fe films ( residual stress data for the 65Co15Ni20Fe film is taken from literature (18)). Small additions of saccharin to plating solutions can alter the residual stress of nickel from tensile to compressive.

### Hard Magnetic Materials in MEMS

Although soft magnetic materials can be used to produce high-force actuators and sensitive magnetometers, hard magnetic or permanent magnetic materials would be more appropriate in some cases. For example, hard magnetic materials with a high remanence,  $M_r$ , are well suited for bi-directional (push-pull) microactuator applications (17). In addition, microactuators driven by off-chip coils can be activated with lower fields and hence lower power levels if a hard magnetic material is used instead of a soft magnetic material. However, except in a few cases, hard magnetic materials have not been used extensively in MEMS (6). The primary reason for this is the lack of readily available and reliable deposition and micromachining processes. A large variety of hard magnetic materials can be prepared by metallurgical processes (e.g. sintering, pressure bonding, injection molding, casting, extruding, and calendaring), vacuum processes (e.g.



evaporation, sputtering, MBE, CVD) and electrochemical processes (e.g. electroless deposition and electrodeposition).

Magnetic Properties of Hard Magnetic Materials. To date, most hard magnetic materials have been alloys based on cobalt because its hcp crystalline structure is highly anisotropic. Electrochemically, Co-based alloys containing P, As, Sb, Bi, W, Cr, Mo, Pd, Pt, Ni, Fe, Cu, Mn, O and H have been deposited. Alloying elements tend to concentrate at the grain boundaries. Thus, the resulting structure consists of isolated magnetic Co grains surrounded by non-magnetic or weakly magnetic boundaries (19). Such microstructural formations increase the energy barrier for magnetic realignment of the domains and thereby increase the overall coercivity  $H_C$  of the films, making them magnetically hard. Park et al. observed that the addition of phosphorus into electrodeposited CoNi films produced nanocrystalline films with a modified crystal structure, increasing the energy barriers required for the magnetic alignment of the CoNi grains (20). Elements that are exceptions to this rule are Pd and Pt, which are readily alloyed with Co or CoNi and instead have the effect of increasing the magnetocrystalline anisotropy (21). Luborsky's experiments with electrodeposited Co and CoNi containing P, As, Sb, Bi, W, Mo and Cr as alloying elements showed that the concentration of the alloying element required for maximum coercivity decreased in the following orders  $P > As > Sb > Bi$  and  $W > Mo > Cr$  (19). Also, as expected, the magnetic saturation  $M_S$ , decreases with increasing content of the non-magnetic alloying element. Low alloy concentrations of phosphorus and tungsten, however, have resulted in films with high coercivity with yet having relatively high  $M_S$ .

Promising hard magnetic thin film materials include CoPt and FePt due to their high magnetocrystalline anisotropy and magnetic saturation (21). Specifically,  $L_{10}$  ordered phase materials (Co50Pt50 and Fe50Pt50) show extremely high coercivities ( $>10,000$  Oe) (22). Most investigations of CoPt and FePt magnetic thin films were conducted using vacuum-based processes [e.g. MBE (23) and sputtering (22-25)], in which CoPt and FePt were deposited as multilayered structures and then annealed to produce ordered phases. A major disadvantage of these deposition methods for some magnetic MEMS applications is the requirement for high-temperature post-annealing processes (e.g. 500-700 °C). Integrated circuits and some materials commonly used in MEMS (e.g. Al, polymer, etc.) do not survive at these temperatures. Although Farrow and Marks report that by electrochemically charging the transition metal alloy films with hydrogen, one can minimize the effects of the annealing process (25), it is nevertheless still a problem.

CoPt and Co/Pt multilayers can be electrodeposited from various plating solutions at or near room temperature (26-30). Cavallotti et al obtained hard magnetic Co-Pt electrodeposits with a coercivity that ranged from 4000 to 2000 Oe for film thicknesses from 50 nm to 10 microns (30).

Myung *et al.* also studied various electrodeposited hard magnetic Co-based alloys and found promising hard magnetic properties. Coercivity in the direction parallel to the film decreased in the following sequence:  $CoPtP > CoNiP \approx CoP > CoMnP > CoW$ . In the perpendicular direction, coercivity decreased in the sequence of  $CoPtP > CoNiP \approx CoMnP > CoP > Co/Cu$  multilayers  $> CoW$  (31). Figure 6 shows how the coercivity of different phosphorus containing alloys varies with the P content. Non-Ni containing

alloys, such as CoP, exhibit increasing coercivity with increasing P incorporation into the alloy. On the other hand, Ni containing alloys show this increase in coercivity with increasing amount of P in the alloy, only for low P concentrations. As more phosphorus is added to these alloys, the coercivity reaches a maximum, followed by a significant reduction at high P concentrations. The highest coercivities were observed for the 85Co15NiP films. Figure 7 shows the hysteresis loops (fig. 7a) and 2<sup>nd</sup> quadrant B-H curves (fig. 7b) for these various electrodeposited alloys.

Corrosion Resistance of Hard Magnetic Materials. As shown in Figure 2, electrodeposited cobalt is much more susceptible to corrosion attack than either nickel or permalloy. Non-magnetic alloying elements (e.g. phosphorus, tungsten, manganese) are not beneficial in this respect and can significantly lower the corrosion resistance of these alloys. Furthermore, it has been observed that some of these hard magnetic materials are etched away during the photoresist removal step during lithographic patterning. It is therefore recommended that these magnetic materials have an overcoat of high corrosion resistance materials (e.g. Au, Pt, Ni) in order to prevent their dissolution during MEMS processing.

Residual Stress of Hard Magnetic Materials. In general, hard magnetic alloys become mechanically brittle and hard as their magnetic hardness increases. Therefore, this reduction in mechanical ductility results also in hard magnetic materials having high residual stress. Figure 8 shows the residual stress of electrodeposited CoNiP and CoP films plotted as a function of the P content. Electrodeposited CoNiP and CoP films have a much higher (above 200 MPa) tensile residual stress than pure nickel or cobalt films and show a maximum in the residual stress when the electrolyte baths concentrations of NaH<sub>2</sub>PO<sub>2</sub> are in the range of 1 to 2 g/L. In order to lower the residual stress while yet maintaining high coercivity, composite films consisting of these highly tensile magnetic films sandwiched between compressive films can be electrodeposited.

## CONCLUSION

Magnetic materials, particularly ferromagnetic materials, have many uses in MEMS. Although soft magnetic materials have found the greatest utility in MEMS, improved processes for integrating hard magnetic materials with MEMS are being developed. These electrochemical processes and resulting properties of the deposited magnetic films must be further optimized for use in high-force microactuators and low-power microsensors.

## ACKNOWLEDGEMENT

The authors wish to acknowledge his collaborators, including T. George, D. Wiberg, K.-ah Son, B. Eyre, O. Orient, D. Miller from JPL and K. Nobe, M. Schwartz, B.-Y. Yoo and J.W. Judy from UCLA. This work was supported by the NASA Code-R and DARPA MEMS Program DABT63-99-1-0020.

## REFERENCES

1. J. W. Judy, R. S. Muller and H. H. Zappe, *IEEE J. Microelectromechanical Systems*, 4, 162 (1995).

2. J. W. Judy and R. S. Muller, *Sensors and Actuators (Physical A)*, **A53**, 392 (1996).
3. J. W. Judy and R. S. Muller, *IEEE J. Microelectromechanical Sys.*, **6**, 249 (1997).
4. C. H. Ahn and M. G. Allen, *IEEE Trans. Ind. Electron.* **45**, 866 (1998).
5. T. M. Liakopoulos, M. Xu and C. H. Ahn, *Technical Digest Solid-State Sensor and Actuator Workshop*, Hilton Head Island, SC, USA, 19 (1998).
6. T. S. Chin, *J. Magn. Magn. Mater.* **209**, 75 (2000).
7. P. C. Andricacos and N. Robertson, *IBM J. Res. Develop.*, **42** 671 (1998).
8. S.H. Liao, *IEEE Trans. Mag.*, **26**, 328 (1998).
9. N. V. Myung and K. Nobe, *J. Electrochem. Soc.* **148**, C133 (2001).
10. D. Kim, D.-Y. Park, B.Y. Yoo, P.T.A. Sumodjo and N.V. Myung, *Electrochim. Acta*, *in press* (2002).
11. T. Osaka, T. Sawaguchi, F. Mizutani, T. Yokoshina, *J. Electrochem. Soc.*, **146**, 3295 (1999).
12. H.H. Uhlig, "*Corrosion Handbook*" John Wiley and Sons, Inc., pp. 194 (1948).
13. G. S. Frankel, V. Brusic, R. G. Schad and J. -W. Chang, *Corr. Sci.*, **35**, 63 (1993).
14. T. Yokoshima, M. Kaseda, M. Yamada, T. Nakanishi, T. Momma, T. Osaka, *IEEE Trans. Magn.* **35**, 2499 (1999).
15. J. W. Dini, "*Electrodeposition - The Materials Science of Coating and Substrates*", Chap. 9, Noyes Publications, (1992).
16. Yu. K. Vyagis, A. I. Bodnevas, and Yu. Matulis, *Protection of Metals*, **1**, 468 (1965).
17. I. Tabakovic, V. Inturi, S. Riemer, *J. Electrochem. Soc.*, **149**, C18 (2002).
18. H. J. Cho, S. Bhansali, and C. H. Ahn, *J. Appl. Phys.*, **87**, 6340 (2000).
19. F. E. Luborsky, *IEEE Tran. Magn.*, **6**, 502 (1970).
20. D.-Y. Park, N.V. Myung, M. Schwartz, and K. Nobe, *Electrochim. Acta*, **47**, 2893 (2002).
21. R. M. Bozorth, *Ferromagnetism*, D. Van Nostrand (1963).
22. K. R. Coffey, M. A. Parker and J. K. Howard, *IEEE Trans Magn.* **31**, 2737 (1995).
23. C. H. Lee, R. F. C. Farrow, C. J. Lin and E. E. Marinero, *Phys Rev. B.* **42**(7) 11384 (1990).
24. P. F. Garcia, Z. G. Li, and W. B. Zeper, *J. Magn. Magn. Mater.*, **121**, 452 (1993).
25. R. F. Farrow and R. F. Marks, *U. S. Patent #5,792,510*.
26. Y. Jyoko, S. Kashiwabara, Y. Hayashi, W. Schwarzacher, *J. Magn. Magn. Mater.*, **198/99**, 239 (1999).
27. J. Horkans, D. J. Seagle, and C. H. Chang, *J. Electrochem. Soc.*, **137**, 2056 (1990).
28. M. Monew, I. Krastev, and A. Zielonka, *J. Phys. Cond. Matter*, **49**, 10033 (1999).
29. V. Tutovan and V. Georgescu, *Thin Solid Films*, **61**, 133 (1970).
30. P. L. Cavallotti, N. Lecis, H. Fauser, A. Zielonka, J. P. Celis, G. Wouters, J. Machado da Silva, J. M.B. Oliveira and M. A. Sa, *Surf. Coat. Technol.*, **105**, 232 (1998).
31. N. V. Myung, D.-Y. Park, M. Schwartz, K. Nobe, H. Yang, C.-K. Yang, J. W. Judy, *Proc. Electrochemical Soc.* **PV2000-29**, 506 (2000).

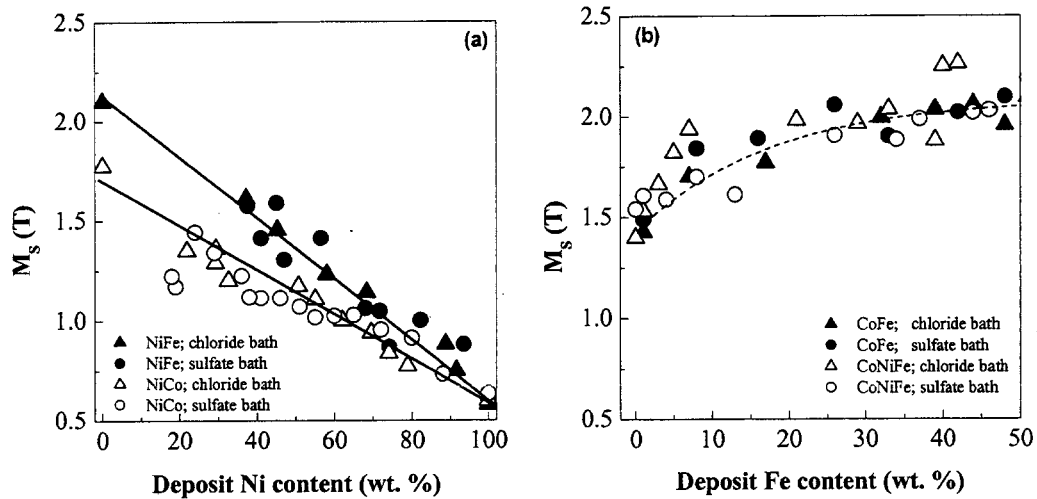


**Figure 1.** Magnetic Saturation of electrodeposited (a) NiFe, NiCo, and (b) CoFe, and CoNiFe films [Ref. 8,9].

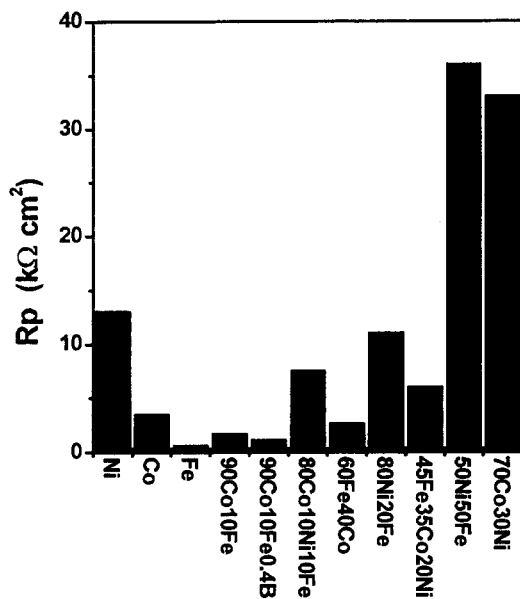


**Figure 2.** Comparison of corrosion resistances of iron group alloys in 0.5 M NaCl after 1 hour immersion.

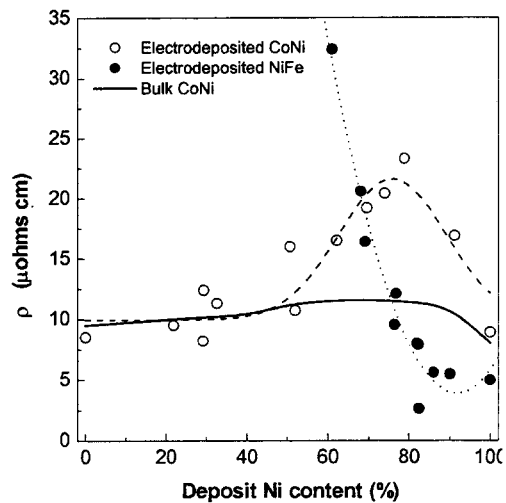


**Figure 3.** Electrical resistivity of NiFe and CoNi thin films electrodeposited from chloride baths and bulk CoNi.

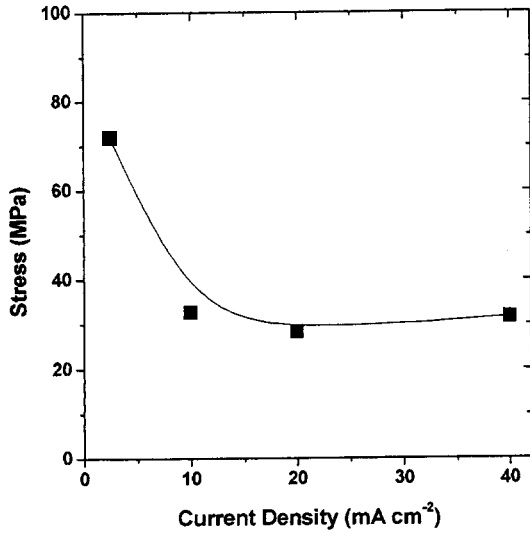


**Figure 4a.** Intrinsic stress of electrodeposited Ni from 1 M Ni sulfamate bath, pH = 4.0, Temp = 60 °C.

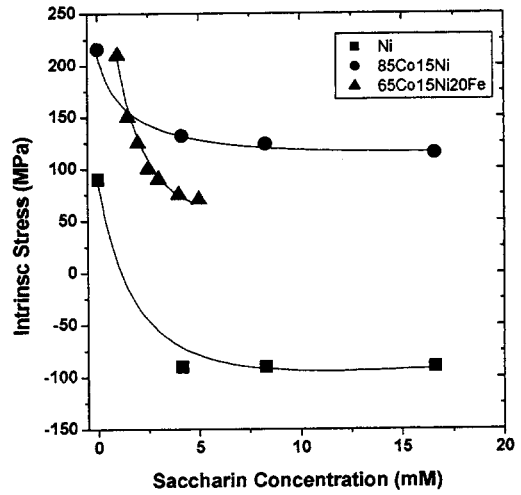


**Figure 5.** Residual stress of electrodeposited Ni, 85Co15Ni, and 65Co15Ni20Fe films. Ni and 85Co15Ni were electrodeposited from sulfamate baths, 65Co15Ni20Fe film data is from literature (17).

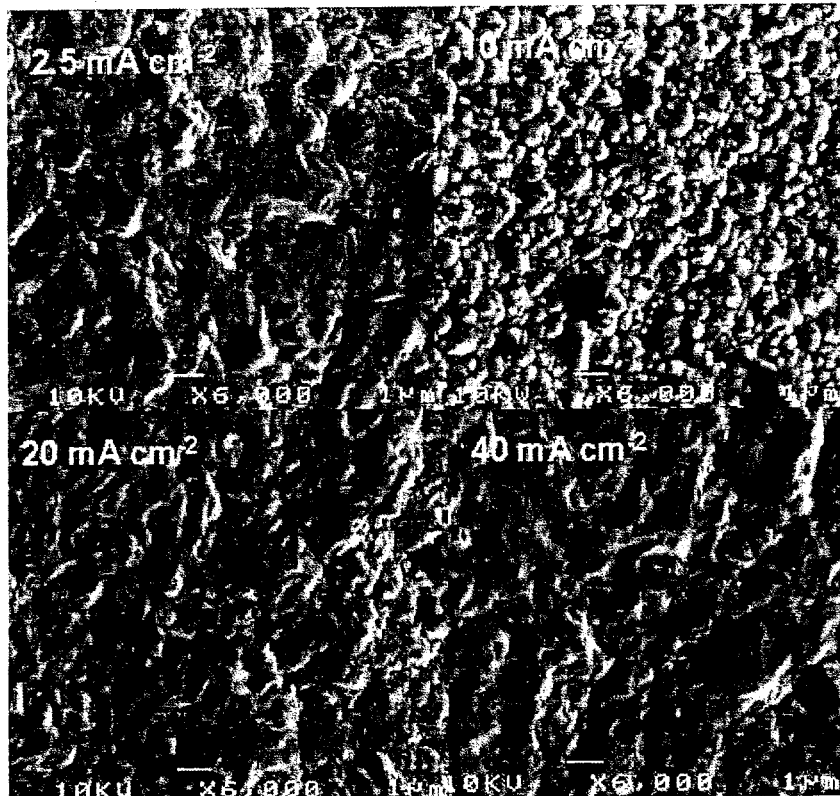


**Figure 4b.** SEM micrographs of Ni films electrodeposited from a 1 M Ni sulfamate bath, pH = 4.0, Temp = 60 °C.

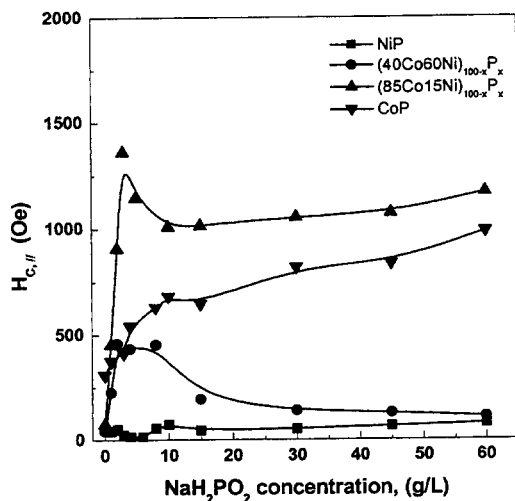


**Figure 6.** Coercivity of electrodeposited NiP 40Co60NiP, 85Co15NiP and CoP films: All films were electrodeposited from chloride baths.

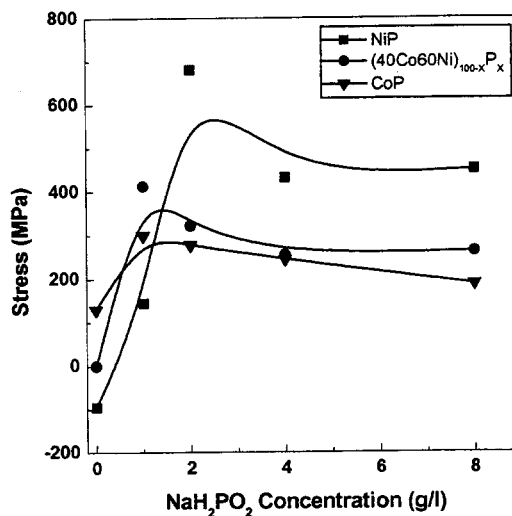
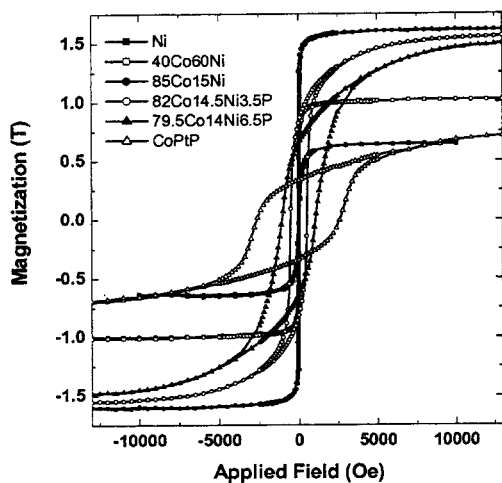


**Figure 8.** Residual stress of electrodeposited NiP 40Co60NiP, and CoP films: All films were electrodeposited from chloride baths.

a)



b)

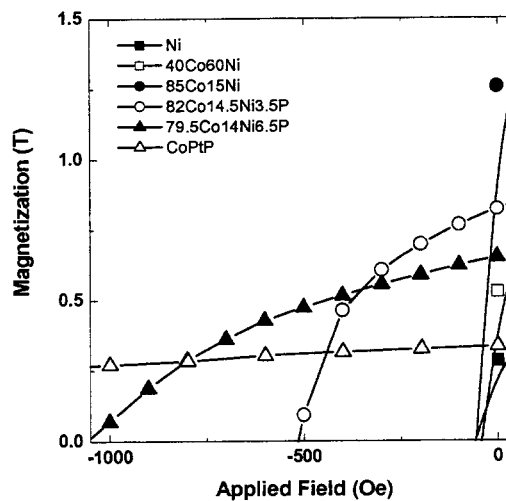


**Figure 7.** Hysteresis loop (a) and 2<sup>nd</sup> quadrant B-H curves for various electrodeposited magnetic alloys